PROCEEDINGS OF SPIE

SPIEDigitalLibrary.org/conference-proceedings-of-spie

Continuous detection of particles on a rotating substrate during thin film deposition

Rüsseler, Anna Karoline, Balasa, Istvan, Jensen, Lars, Ristau, Detlev

Anna Karoline Rüsseler, Istvan Balasa, Lars Jensen, Detlev Ristau, "Continuous detection of particles on a rotating substrate during thin film deposition," Proc. SPIE 10805, Laser-Induced Damage in Optical Materials 2018: 50th Anniversary Conference, 108051X (19 November 2018); doi: 10.1117/12.2500210

SPIE.

Event: SPIE Laser Damage, 2018, Boulder, Colorado, United States

Downloaded From: https://www.spiedigitallibrary.org/conference-proceedings-of-spie on 08 Dec 2020 Terms of Use: https://www.spiedigitallibrary.org/terms-of-use

Continuous detection of particles on a rotating substrate during thin film deposition

Anna Karoline Rüsseler*[a], Istvan Balasa[a], Lars Jensen[a], Detlev Ristau[b,a]
[a]Laser Zentrum Hannover e.V., Hollerithallee 8, 30419 Hannover, Germany;
[b]Gottfried Wilhelm Leibniz Universität Hannover, Welfengarten 1, 30167 Hannover, Germany

ABSTRACT

Particles, which contaminate the substrate during thin film deposition, are prone to cause irremovable defects and demand special attention in the field of high precision laser optics as they can lead to localized absorption and laser damage. In this contribution, we present a camera based fully in-vacuum device which continuously monitors the coating surface of a transparent test substrate under dark field illumination. We show the possibilities of this setup regarding the sensitivity to small particles (diameter 1 µm). As the first operational test of the particle monitor, singe layers of HfO_2 are grown on fused silica. By analyzing the evolution of the scattering intensity of the particles, we derive their position in the substrate-coating-system. Therefore, this in situ particle detection concept can deliver data on which process step is responsible for particle generation in multilayer films and aims to be a tool to minimize coating defects.

Keywords: thin films, defects, particles, laser damage, in situ monitoring, coatings, sputter deposition

1. INTRODUCTION

On coated optics, particles and other defects can cause localized absorption, which is of special interest for laser applications: Especially for high power lasers in the nanosecond regime, absorption centers induce a local heating effect and can lead to thermal damage[1, 2]. In addition, not only considering damage phenomena, a broad variety of deficiencies such as delamination, increased scatter losses, or wavefront distortions can be attributed to unwanted particle inclusions in the coating. Particles, which are embedded in the coating, are particularly problematic because they either cannot be removed, or they are leaving a defect upon removal by standard cleaning procedures. As they are overcoated by thin film material, even small particles can initiate the formation of larger defects by nodular growth[3-5]. Therefore, minimizing the particle generation during the coating process is an important objective in the optical coatings industry.

In order to avoid these problems, efforts have been made to better understand the causes of particle contamination in thin films by in situ metrology. The formation and transport of particles in plasma processes is the subject of several studies which use laser light scattering, recorded through a window[6-9]. The laser light scattering method was also applied to the magnetron sputtering process[10, 11]. In these studies it is shown, that one source of particles during magnetron sputter deposition is the ejection of filaments, which grow on the sputter target, into the vacuum chamber. Furthermore, there are approaches to monitor particle generation by measuring the scattered laser light in the defined volume of a particle detector, placed inside the vacuum chamber[12, 13]. Recently, we reported on another camera based in situ particle detection concept in a magnetron sputter deposition chamber, which utilizes dark field LED illumination through a window: For a direct monitoring of the substrate surface, the rotation of the substrate plate was stopped multiple times during the deposition and the test substrate was positioned reproducibly to a camera[14]. With this time resolved monitoring, we documented a linear increase of the particle contamination with an increasing layer thickness of a Ta_2O_5 single layer during the first 500 nm of deposition. For single layers of SiO_2, we also observed an increase of particles over layer thickness. The observed particle densities of the coated samples were compared to high resolution ex situ laser scanning microscopy and showed good agreement.

However, to adapt to different coating chamber geometries, which do not necessarily allow a direct view of the substrate through a window, we hereby present a modified approach to the latter monitoring concept. This fully in-vacuum in situ monitoring system is decoupled from the atmospheric side and has its own power supply. It is mounted on the substrate

*a.ruesseler@lzh.de; www.lzh.de

Laser-Induced Damage in Optical Materials 2018: 50th Anniversary Conference, edited by Christopher Wren Carr, Gregory J. Exarhos, Vitaly E. Gruzdev, Detlev Ristau, M.J. Soileau, Proc. of SPIE Vol. 10805, 108051X
© 2018 SPIE · CCC code: 0277-786X/18/$18 · doi: 10.1117/12.2500210

Downloaded From: https://www.spiedigitallibrary.org/conference-proceedings-of-spie on 08 Dec 2020
Terms of Use: https://www.spiedigitallibrary.org/terms-of-use

plate and co-rotates with a transparent test substrate, viewing the coating surface through the substrate's volume. Dark field images are automatically captured and saved on a single board computer without the need for additional process steps. Therefore, this detection concept minimizes the intervention in the actual coating process and is particularly interesting for production quality control.

2. EXPERIMENTAL

2.1 In situ detection

To realize dark field illumination, the camera must be oriented perpendicular to the substrate surface while the light is incident at an oblique angle, so that the specular reflection of the surface passes the camera lens (see figure 1.a). Inhomogeneities on the surface, such as particles, which are large compared to the wavelength of the light scatter some of the incident light into all directions[15] and thus partly in the direction of the camera. Therefore, defects appear on the image as brighter dots against the darker background and can be evaluated by automated particle analysis software based on edge detection (5x5 Sobel[16]), which has been implemented in GNU Octave[17]. The illumination consists of an array of four blue LEDs (peak wavelength 466 nm, 25 nm full width at half maximum). Each of the four LEDs generates 21.5 mW at 466 nm. A band pass filter for the wavelength of the LEDs in front of the camera further increases the signal to noise ratio of the detection by blocking interfering light, which is generated, for example, by the process plasma. The camera and its lens are positioned close to the substrate, at a working distance of 20 mm, to reach high resolution and good detection capability.

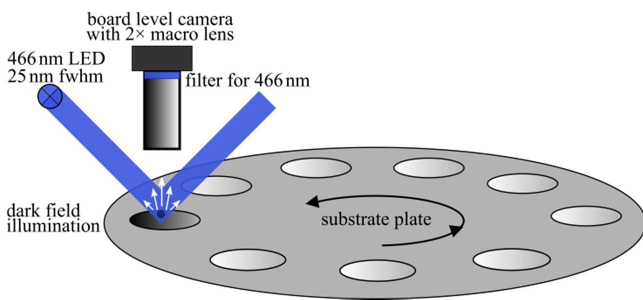

Figure 1.a. Schematic of the dark field detection principle.

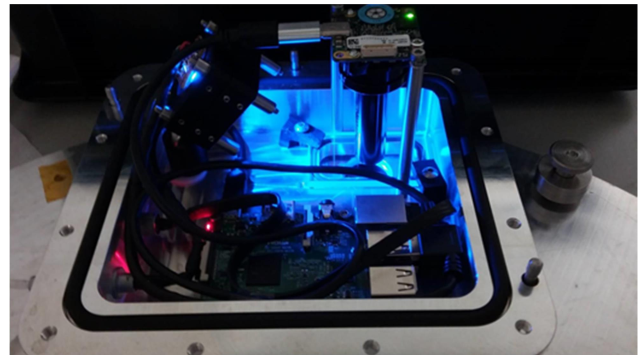

Figure 1.b. Photo of the inside of the particle detection module, showing the components labeled in figure 1.a and the single board computer in the front.

In order to realize a versatile detection concept, which can be implemented into a variety of IBS chambers, we constructed a very compact setup. The camera and the illumination are housed in a specially designed, O-ring sealed aluminum housing with a window at the bottom, together with a single board computer for camera control and image storage. Figure 1.b shows a photo of the setup. To balance the weight distribution, the power supply is located in its own housing on the opposite side of the substrate plate (see figure 2), and a tare weight is also used. No cooling is required for the housings, because the IBS process operates at moderate temperatures (typically $< 80\,°C$). Additionally, the thermal contact from the housings to the substrate plate, which is hit by the plasma, is minimized. During two hours of continuous deposition, the temperature inside the housings, generated by the deposition process alone, did not exceed 39 °C.

For the experiments, fused silica substrates with a diameter of 25.4 mm were used. The surface quality of these substrates was specified by the manufacturer to fulfill the scratch / dig requirement 60 / 40 according to MIL-PRF-13830B-1997. Before deposition, the substrates were cleaned in an automatic cleaning line, which combines ultrasonic cleaning and cleaning agents. The HfO_2 deposition was performed using an oxidic sputtering target and oxygen inlet. The single layers were deposited on a time-controlled basis.

Downloaded From: https://www.spiedigitallibrary.org/conference-proceedings-of-spie on 08 Dec 2020
Terms of Use: https://www.spiedigitallibrary.org/terms-of-use

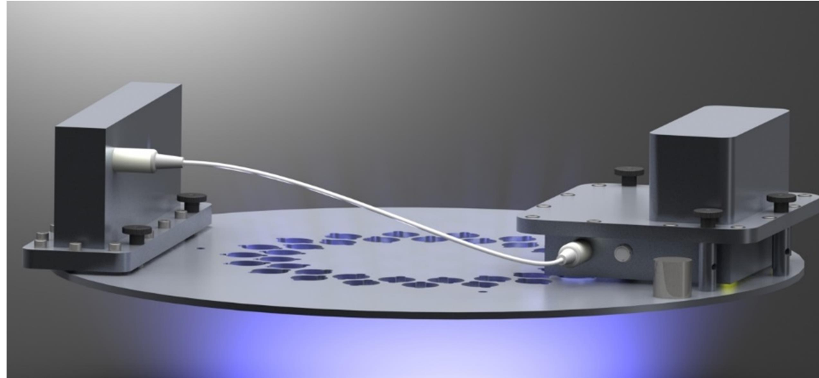

Figure 2. Rendering of the in situ particle monitor. The compartment on the left hand side contains the power supply and the compartment on the right hand side is the detection module as shown in figure 1.b. The test substrate is located directly below the window in the bottom of this compartment. Parallel to the particle measurement, further substrates can be coated on the standard radii of the substrate plate.

The individual components of the particle monitor were selected to be cost-efficient on the one hand and small on the other, in order to take account of the space constraints in the vacuum chamber. A 6 Megapixel board level monochromatic camera is used, the quantum efficiency of this camera is specified by the manufacturer to be >70% at 466 nm. There are two options for the camera lens, each of which optimizes a different aspect of the analysis: High field of view or high resolution. With a compact, commercially available camera lens with a fixed focal length of 12 mm, imaging of the entire diagonal of the 25.4 mm substrate is possible. For achieving higher resolution, a 2× macro lens is used. With the macro lens, the analyzed section of the sample is approximately $(4.4 \times 2.8)\,mm^2$.

To characterize the detection limit of the particle monitor, a particle size reference was manufactured. On the size reference, laser ablation defects are arranged in rows, with defect diameter decreasing from row to row. Figure 3 shows a section of the in situ image of the size reference taken using the high resolution macro lens. The resolution of the image in the focal plane is calculated by the known distance between the defects of 500 µm. This distance is displayed on 340 pixels in the camera image. It can be seen, that despite this resolution being 1.47 µm, the 1 µm diameter ablations can still be detected due to their stray light cone in the dark field illumination.

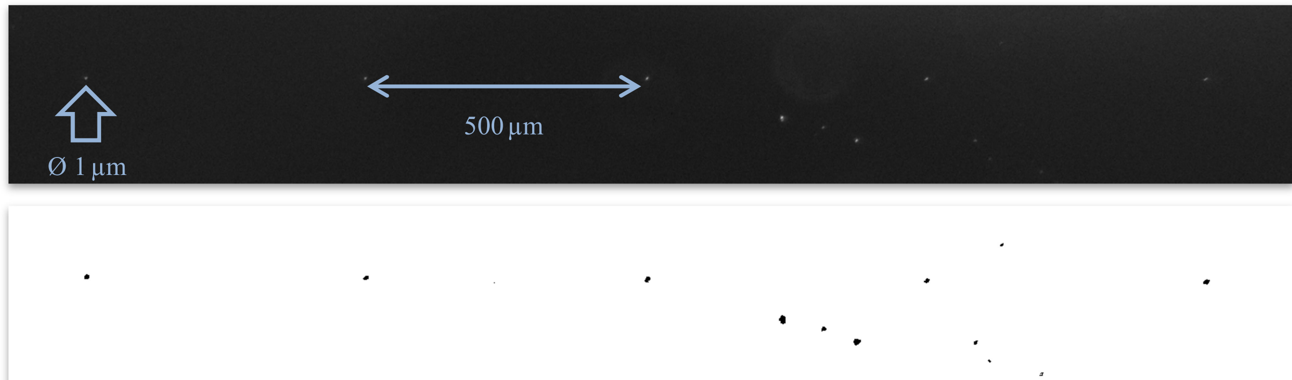

Figure 3. Top: Row of laser ablated defects of known diameter (1 µm) on fused silica, section of in situ image taken with macro camera lens. Additional contamination by dust particles can be seen next to the row. Bottom: Resulting image of the evaluation with the particle analysis software (inverted colors for visibility).

Figure 4 shows evaluated sections of an in situ image of the same size reference, as taken with the higher field of view camera lens. The defects with 2 µm diameter can still be detected.

Downloaded From: https://www.spiedigitallibrary.org/conference-proceedings-of-spie on 08 Dec 2020
Terms of Use: https://www.spiedigitallibrary.org/terms-of-use

Figure 4. Rows of laser ablated defects of known diameter (10 µm, 5 µm, 2 µm) on fused silica, evaluated sections of in situ images, taken with the high field of view camera lens.

2.2 Ex situ microscopy

After deposition, the particle contamination of the samples was examined by dark field microscopy. This is a way to determine the size distribution of the particles. The microscope (Zeiss Axio imager.M2m) images an area of about (1.7×1.4) mm² at 100× magnification, and scans the sample area. 137 images were considered, resulting in an analyzed area of approximately 338 mm². The estimation of the measured particle size was corrected using a NIST traceable standard for surface defects. Comparing the real size of these standardized defects to their measured size, an empirical size correction function was determined: A sigmoid function with values ≤ 1, which corrects the size downwards because the particles are measured too large.

3. RESULTS AND DISCUSSION

3.1 In situ monitoring data

The automatic image analysis script, based on edge detection, is used to count the particles as well as to record the detected scattering intensity of individual particles. The latter is performed by plotting the averaged grayscale value of the pixels, which are detected to belong to a particle, over the layer thickness. An oscillation in the brightness is observed, as can be seen in figure 5 for two exemplary particles. For comparison, the reflection of the thin film system at 466 nm, calculated by the software SPEKTRUM[18], is plotted below the graph with the in situ data points. The refractive index of HfO_2 was calculated from spectrometer measurements on layers of different thicknesses to be $n_{HfO_2} = 2.0842$ at 466 nm.

The in situ measurements reveal a positive correlation between the detected brightness of the particles and the reflection of the thin film system in the direction of the camera at the detection wavelength of 466 nm. At the reflection maxima, the brightness of the particles is enhanced by the thin film.

Downloaded From: https://www.spiedigitallibrary.org/conference-proceedings-of-spie on 08 Dec 2020
Terms of Use: https://www.spiedigitallibrary.org/terms-of-use

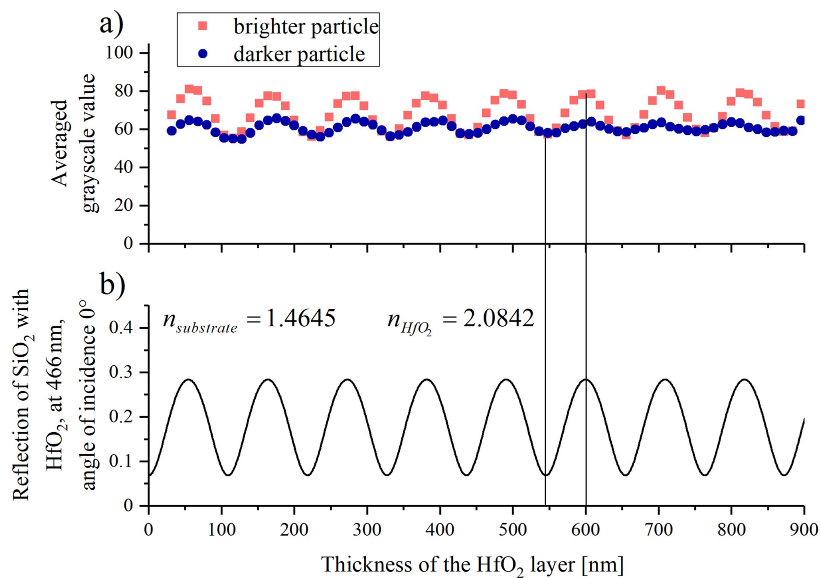

Figure 5. a) Evolution of grayscale value of exemplary particles on the in situ images, corresponding to their detected scattering intensity. The values are plotted over the layer thickness of the HfO_2 thin film. b) Calculated reflection of the HfO_2 thin film on the fused silica substrate ($n_{SiO_2} = 1.4645$). The vertical lines connecting the graphs are a guide to the eyes.

It has been shown in a previous paper on time resolved particle detection in a magnetron sputter process, that more particles are detectable by a dark field setup at the reflection maxima of the thin film system at the illumination wavelength and normal incidence[14]. In that publication, the evolution of particles during the sputtering of SiO_2 and Ta_2O_5 was evaluated and an oscillation in particle count over layer thickness was observed, together with a linear increase of particles with increasing thickness of the single layer. Our measurements with the new in situ particle monitor confirm that a possible explanation for this oscillation is the reflection of the thin film enhancing the scattering intensity of particles, so that they exceed the detection threshold of the image analysis software at reflection maxima.

The particles can generally be assumed to be free-form defects. However, to model the scattering and the correlation to the reflection, we consider the case of a spherical particle. The scattering behavior of spheres is described theoretically by the Mie solution to Maxwell's equations[19]. The Mie solution is valid for particles, which are equal to or larger than the wavelength of the incident light, which is the case for the particle monitor setup. The program MiePlot v4.6.13[20] was used to simulate the angular scattering intensity distribution according to the Mie theory. The simulation for an exemplary particle of SiO_2, which is embedded in the HfO_2 thin film, is shown in figure 6.

The angular Mie scattering intensity of particles in the micrometer range, illuminated by visible light, has a pronounced maximum in the forward direction and the scattering into the rest of the forward half-sphere exceeds the scattering into the rear half-sphere by orders of magnitude. If a particle is located directly on the substrate surface and is overcoated by thin film material, its detectability in the in situ particle monitor setup can be increased: For the reflection maxima for normal incidence, some of the higher intensity forward scattering is located in the field of view of the camera. In the literature, the scattering behavior of overcoated microspheres was compared to the reflection of multilayers on planar substrates and it was found that for cases like the one shown in figure 6, the periodicity of the reflection maxima with increasing layer thickness is similar to the planar case[21]. Furthermore, for free-form defects with flat areas, the layer thickness on the particle is assumed to be equal to the thickness on the planar substrate. Thus, the correlation seen in figure 5 indicates the position of these particles in the thin film system to be directly on the substrate surface or below the surface.

Downloaded From: https://www.spiedigitallibrary.org/conference-proceedings-of-spie on 08 Dec 2020
Terms of Use: https://www.spiedigitallibrary.org/terms-of-use

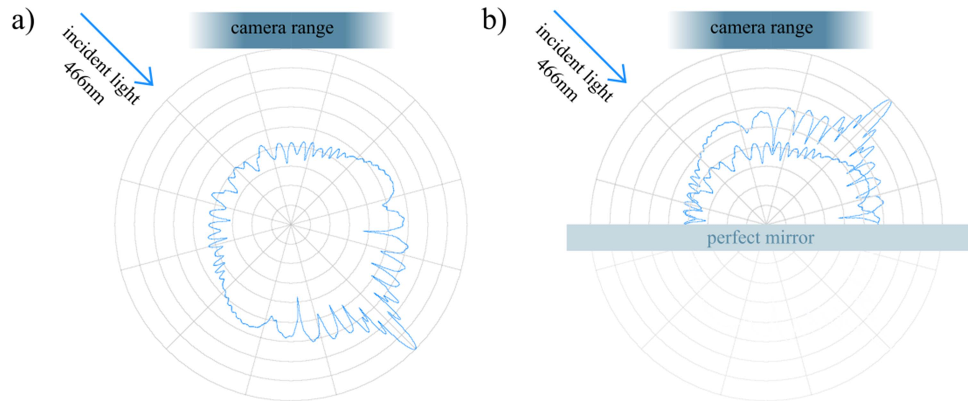

Figure 6. a) Polar plot of angular Mie scattering intensity at 466 nm of a sphere (Ø 5 µm) of SiO_2 embedded in HfO_2, created using [20]. The particle is in the center of the plot, the radial coordinate is in logarithmic units. Incident light and detection range of the camera are indicated above the plot. b) Illustrating the effect of a reflecting surface: high intensity forward scattering partly reaches the camera.

3.2 Microscopy data

The in situ particle monitor can detect particles in the lower micrometer size range, down to 1 µm. The single layer coatings of HfO_2 were analyzed ex situ, to investigate the size range of particles typically occurring on the coated samples. An exemplary resulting size distribution for particles, starting from 1 µm diameter, is shown in figure 7.

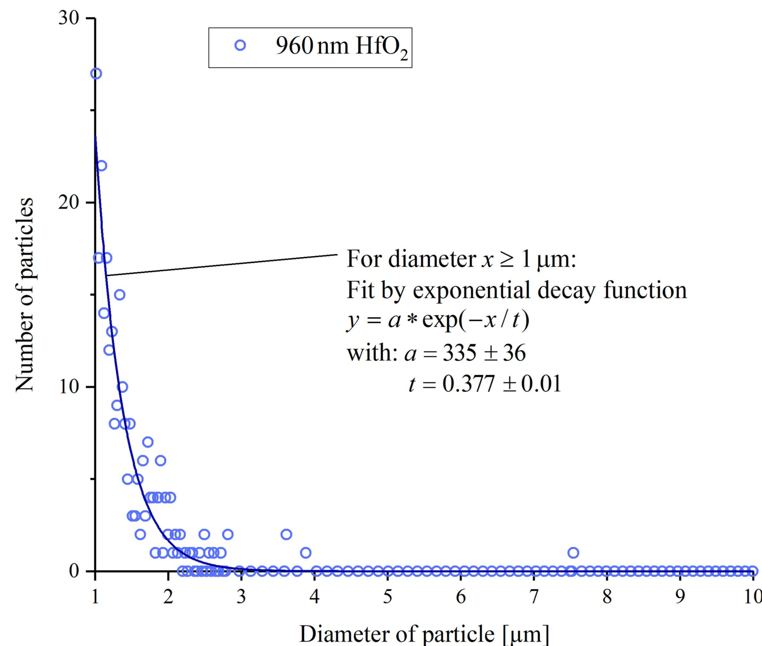

Figure 7: Size distribution of particles ≥ 1 µm on an exemplary coated sample as found by ex situ dark field microscopy (100× magnification, analyzed area of sample ~338 mm^2). The data was fitted using an exponential decay function.

In accordance with literature, the majority of particles found on the samples is small (e.g. <2 µm in diameter)[22]. The size distribution roughly follows an exponential decay with increasing defect size. It must be taken into account that the number of particles can only assume integer values and that a description using an exponential function can at best provide a statistically expected value. In addition, the description with an exponential decay is applicable in the

Downloaded From: https://www.spiedigitallibrary.org/conference-proceedings-of-spie on 08 Dec 2020
Terms of Use: https://www.spiedigitallibrary.org/terms-of-use

displayed range of particle sizes and the size distribution for even smaller particles (<< 1 µm) cannot be inferred directly from the observations in the micrometer particle range.

4. CONCLUSIONS

With the presented fully in-vacuum, in situ particle detection concept, contamination and defects on the substrate can be detected and monitored throughout the ion beam deposition process without additional process steps. Through the continuous detection, process steps can be identified, that are the main contributor for particle contamination in the growing thin film system. The dark field setup allows detecting small defects and particles by their scattered light: laser ablation defects with 1 µm diameter were detectable. By comparison with high resolution ex situ analysis of coated samples by dark field microscopy, we confirm the presence of particles of these sizes on the coated substrates.

We demonstrated the in situ use of this particle monitor on the basis of single layers of HfO_2. The measured particle scattering intensities reveal a correlation to the reflection of the thin film system when their evolution over the deposition process is monitored. This is in agreement to the dependence of measured particle number on the reflection of the thin film, which has previously been reported. In this context, considerations based on Mie scattering indicate that such a particle is located below the growing layer, directly on or in the substrate.

The measurement principle is aiming to study and correlate the influence of the process parameters to the particle load of the thin film. The practical results that can be generated with this measurement setup and the flexibility regarding the coating plant, in which the system can be used, meet moderate acquisition costs of the equipment required for the setup.

ACKNOWLEDGMENTS

This research was funded by the German Federal Ministry for Economic Affairs and Energy (BMWi) within the Promotion of Joint Industrial Research Programme (IGF) due to a decision of the German Bundestag. It was part of the research project 18590 N by the Association for Research in Precision Mechanics, Optics and Medical Technology (F.O.M.) under the auspices of the German Federation of Industrial Research Associations (AiF).

Supported by:

REFERENCES

[1] Walker, T. W., Guenther, A. H. and Nielsen, P. E., "Pulsed laser-induced damage to thin-film optical coatings-part I: experimental," IEEE J. Quantum Electron., 17(10), 2041–2052 (1981).
[2] Walker, T. W., Guenther, A. H. and Nielsen, P. E., "Pulsed laser-induced damage to thin-film optical coatings-part II: theory," IEEE J. Quantum Electron., 17(10), 2053–2065 (1981).
[3] Guenther, K. H., "Nodular defects in dielectric multilayers and thick single layers," Appl. Opt., 20(6), 1034-1038 (1981).
[4] Liao, B., Smith, D. J. and McIntyre, B., "The formation and development of nodular defects in optical coatings," Laser Induc. Damage Optical Mater.: 1985, 305-318 (1988).
[5] Stearns, D. G., Mirkarimi, P. B., and Spiller, E., "Localized defects in multilayer coatings," Thin Solid Films, 446.1, 37-49 (2004).
[6] Selwyn, G. S., McKillop, J. S. and Haller, K. L., "In-situ Particulate Contamination Studies In Process Plasmas," Proc. SPIE 1185, 86-97 (1990).
[7] Borden, P., Mason, J., Klein, M., "Moving in-situ particle monitoring into manufacturing: a status report," Proc. IEEE/SEMI Int. Semicond. Manuf. Sci. Symp., 75-79 (1991).
[8] Selwyn, G. S., "Optical characterization of particle traps," Plasma Sources Sci. Technol. 340-347 (1994).
[9] Uesugi, F., Ito, N., Moriya, T., Doi, H., Sakamoto, S. and Hayashi, Y., "Real-time monitoring of scattered laser light by a single particle of several tens of nanometers in the etching chamber in relation to its status with the equipment," J. Vac. Sci. & Technol. A: Vac., Surf., Films 16(3), 1189-1195 (1998).
[10] Selwyn, G. S., Weiss, C. A., Sequeda, F., and Huang, C., "Particle contamination formation in magnetron sputtering processes," J. Vac. Sci. & Technol. A: Vac., Surf., Films, 15(4), 2023-2028 (1997).

Downloaded From: https://www.spiedigitallibrary.org/conference-proceedings-of-spie on 08 Dec 2020
Terms of Use: https://www.spiedigitallibrary.org/terms-of-use

[11] Selwyn, G. S., Weiss, C. A., Sequeda, F., and Huang, C., "In-situ analysis of particle contamination in magnetron sputtering processes," Thin Solid Films 317, 85–92 (1998).
[12] Bowling, R. A., and Larrabee, G. B., "Behavior and Detection of Particles in Vacuum Processes," J. Electrochem. Soc., 136(2), 497-502 (1989).
[13] Vergöhl, M., Starke, K. and Plagemann, P., "Partikelarme Beschichtungsprozesse zur Herstellung funktionaler Dünnschichtsysteme für industrielle Anwendungen „PartiPro“ Schlussbericht für den Zeitraum: 01.05.2008 - 31.10.2010," Fraunhofer-Ges. - Veröffentlichungsdatenbank Fraunhofer-Publica, 18-42 (2011).
[14] Rüsseler, A. K., Balasa, I., Kricheldorf, H.-U., Vergöhl, M., Jensen, L. and Ristau, D. "Time resolved detection of particle contamination during thin film deposition," Proc. SPIE 10691, 106910H (2018).
[15] Van de Hulst, H. C., [Light Scattering by Small Particles], Dover Publications, Inc. New York, 103-104 (1981).
[16] Bässmann, H. and Kreyss, J., [Bildverarbeitung ad oculos], Springer-Verlag, 192-195 (2013).
[17] Eaton, J. W., Bateman, D., Hauberg, S. and Wehbring, R., “GNU Octave version 4.2.0 manual: a high-level interactive language for numerical computations,” GNU, 2016, <http://www.gnu.org/software/octave/doc/interpreter> (2016).
[18] Dieckmann, M., SPEKTRUM 32 – Design Software, <www.lzh.de> (2018).
[19] Mie, G., "Beiträge zur Optik trüber Medien, speziell kolloidaler Metallösungen," Ann. Phys. 330, 377-445 (1908).
[20] Laven, P., MiePlot v4.6.13, <http://philiplaven.com/MiePlot.htm> (2018).
[21] Voarino, P., Deumié, C. and Amra, C., "Optical properties calculated for multidielectric quarter-wave coatings on microspheres," Opt. Express, 12(9), 4476-4482 (2004).
[22] Rademacher, D., Fritz, B., and Vergöhl, M., "Origin of particles during reactive sputtering of oxides using planar and cylindrical magnetrons," Appl. Opt., 51(7), 927-935 (2012).

Downloaded From: https://www.spiedigitallibrary.org/conference-proceedings-of-spie on 08 Dec 2020
Terms of Use: https://www.spiedigitallibrary.org/terms-of-use